Supplementary Figures

Supplementary Figure 1. Alignment of FtsZ from *Bacillus subtilis, Escherichia coli*, and four α-proteobacteria. FtsZ sequences were aligned using ClustalW2. CTL is highlighted in green. Mutated residues suppressing the bulging and lysis phenotype in the context of ΔCTL are highlighted in red. *B. subtilis* (BsFtsZ), *E. coli* (EcFtsZ), *Hyphomonas neptunium* (HnFtsZ), *Caulobacter crescentus* (CcFtsZ), *Rickettsia parkeri* (RpFtsZ), and *Magnetospirillum magneticum* (MmFtsZ) sequences are included. Asterisks (*) indicate completely conserved residues, colons (:) indicate residues with conservation of strongly similar properties, and periods (.) indicate residues with conservation of weakly similar properties.

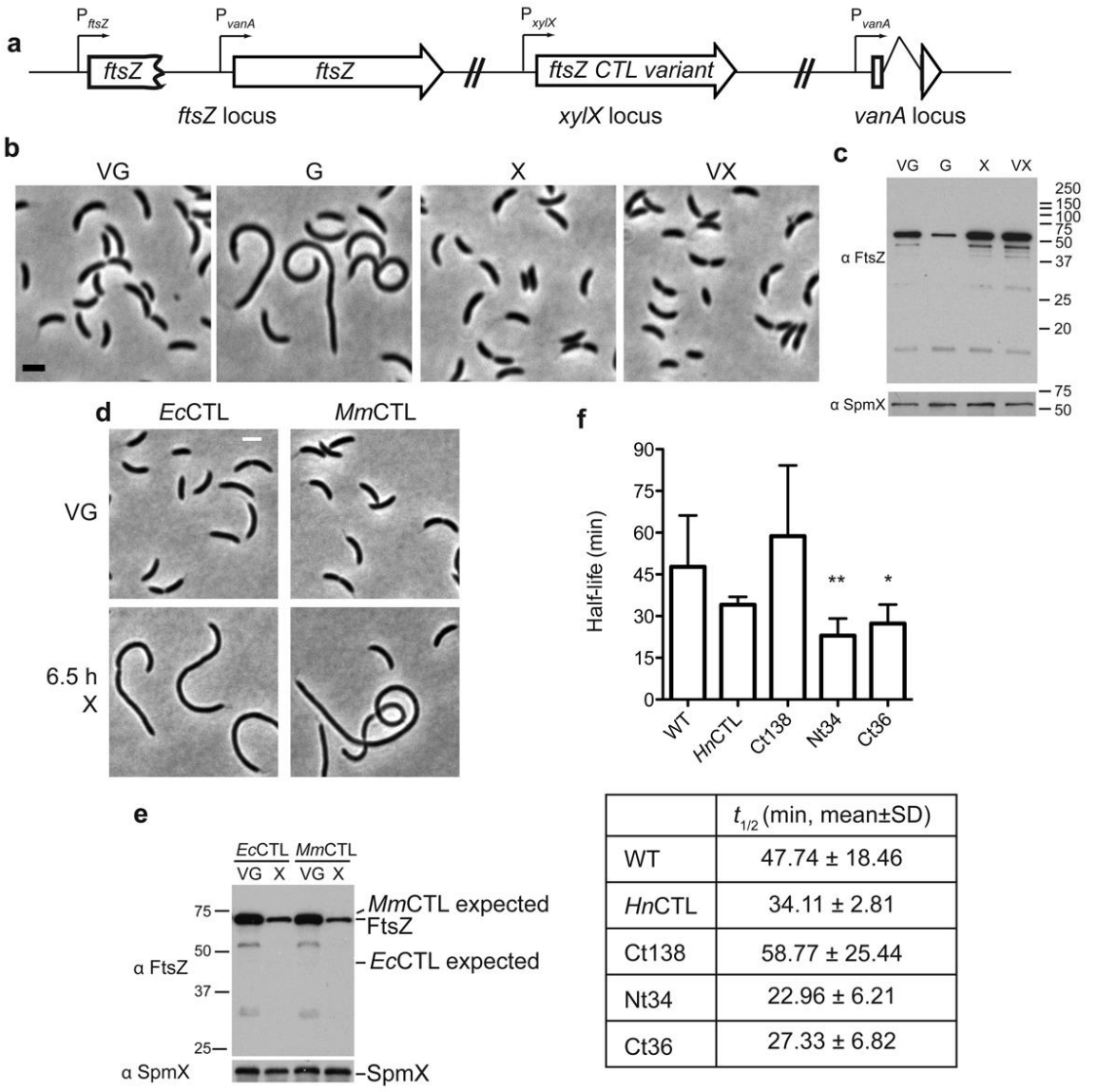

	$t_{1/2}$ (min, mean±SD)
WT	47.74 ± 18.46
*Hn*CTL	34.11 ± 2.81
Ct138	58.77 ± 25.44
Nt34	22.96 ± 6.21
Ct36	27.33 ± 6.82

Supplementary Figure 2. Divergent CTLs do not function in *C. crescentus*. (a) Schematic of the genetic background used to allow differential induction of WT and CTL variants of *ftsZ*. The native copy of *ftsZ* is truncated at the *ftsZ* locus and a vanillate-inducible full-length copy is integrated there. A xylose-inducible copy of the gene encoding the desired CTL variant is integrated at the *xylX* locus. Finally, the *vanA* gene is deleted to prevent metabolism of the vanillate inducer. (b) Phase contrast images of control cells bearing vanillate-induced *ftsZ* and xylose-induced *ftsZ* (WT) grown with vanillate (V),

glucose (G), and/or xylose (X) for 6.5 h. Bar = 2 μm. (c) Immunoblot of lysates from strains in (b) probed with primary antisera raised against FtsZ (top) or SpmX (bottom). Migration positions of molecular weight markers (kDa) are indicated. (d) Phase contrast images of cells bearing vanillate-induced *ftsZ* and xylose-induced CTL variants grown with vanillate and glucose (VG) or xylose (X). Bar = 2 μm. (e) Immunoblot of lysates from strains in (d) probed with primary antisera raised against FtsZ (top) or SpmX (bottom). Migration positions of molecular weight markers (kDa) are indicated. WT FtsZ (54.1 kDa) was depleted, but no protein was detected corresponding to the expected molecular weight of *Ec*CTL (41.5 kDa) or *Mm*CTL (59.4 kDa) when grown in the presence of xylose and in the absence of vanillate for 6.5 h. (f) Bar graph and table of the protein half-lives of the indicated FtsZ variants from strains EG864 (WT), EG769 (*Hn*CTL), EG1000 (Ct138), EG1011 (Nt34), and EG1021 (Ct36). Mean ± standard deviation (s.d.) is plotted. *p*-values indicate significant differences between the means of variants and WT (**: $p<0.005$, *: $p<0.02$, 1-way ANOVA with Dunnett's Multiple Comparison post-test). $n = 6$ biological replicates for all samples except WT ($n = 19$) and Ct138 ($n = 5$).

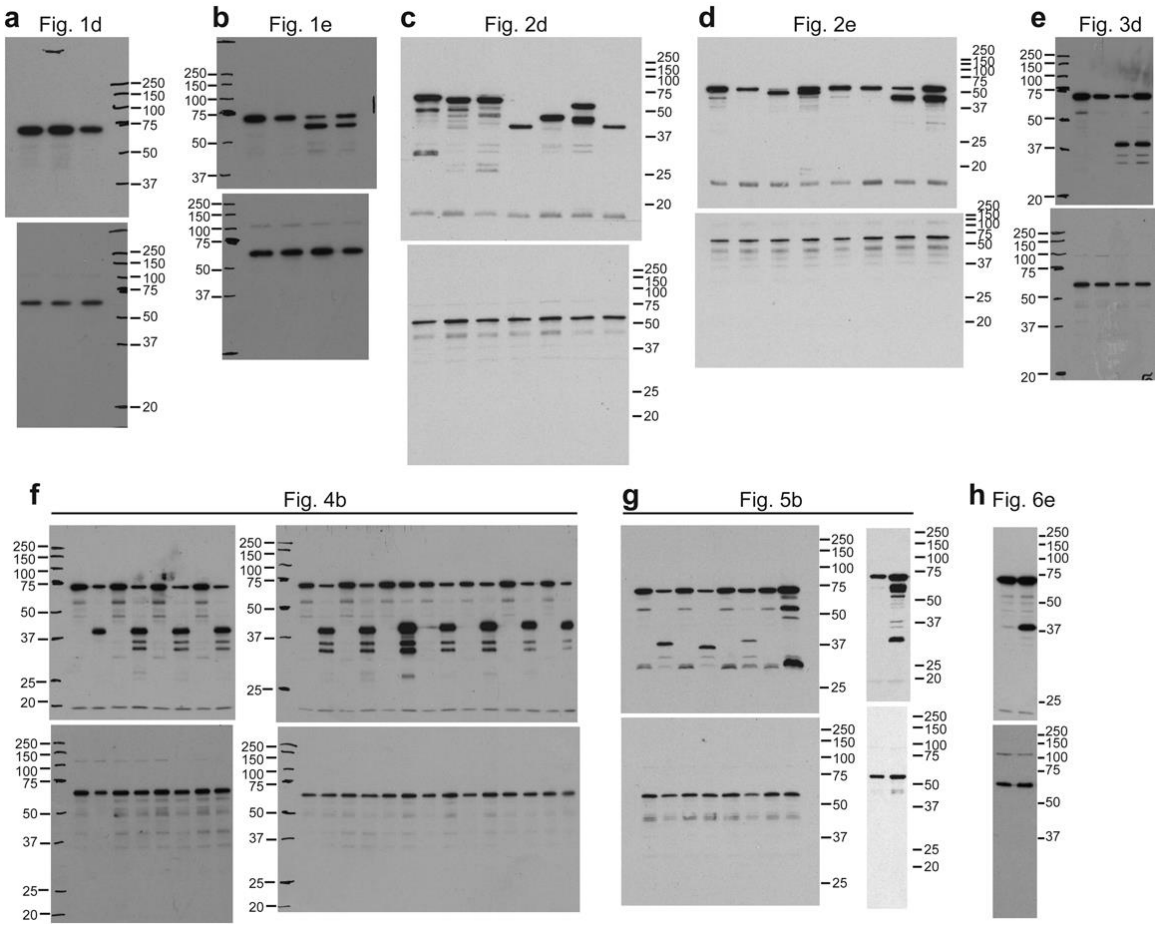

Supplementary Figure 3. Uncropped immunoblots from main figures. (a-h) Scans of developed films from immunoblots used to generate the indicated main figures. In each case, the immunoblot in the top panel was probed with primary antisera raised against FtsZ and the bottom was probed with primary antisera raised against SpmX. Migration positions of molecular weight markers (kDa) are indicated. Sample in each lane is as labeled in the indicated main figure.

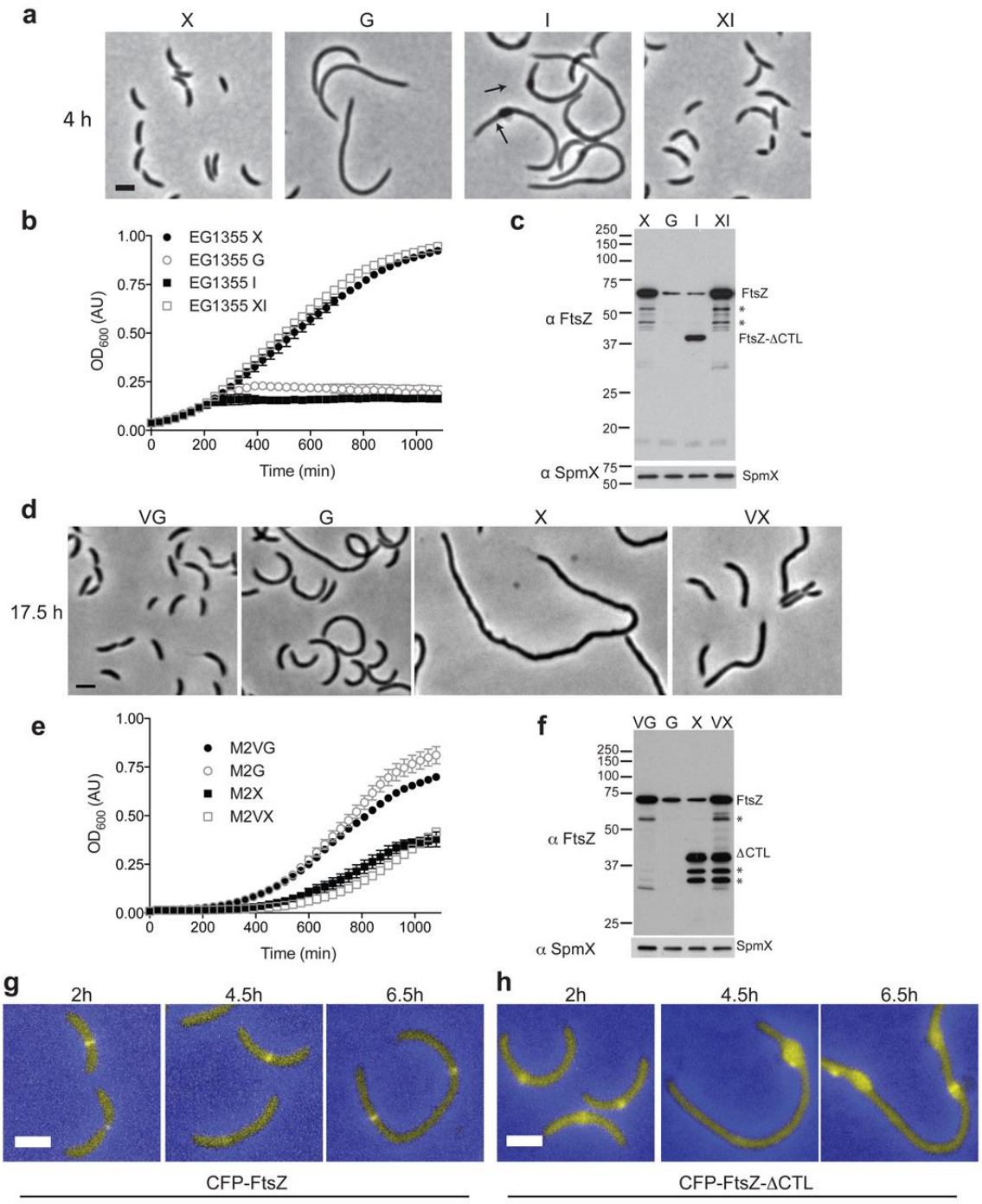

Supplementary Figure 4. ΔCTL production is toxic under a variety of induction conditions and acts locally to induce bulging. (a) Phase-contrast images of cells from strain EG1355, with xylose-induced expression of *ftsZ* and myo-inositol-induced expression of *ΔCTL*. Cells were grown for 4 h in PYE medium with the indicated inducer

(X, xylose; G, glucose; I, myo-inositol) prior to imaging. Bar = 2 µm. (b) Growth of strain EG1355 in PYE with the indicated inducers added at time 0, as monitored by optical density (OD) at 600 nm. Mean ± s.d. from two (X) or three (others) technical replicates is plotted. (c) Immunoblot of lysates of strain EG1355 from (a) after 4 h growth in PYE with the indicated inducers and using FtsZ (top) or SpmX (bottom) antisera. Asterisks indicate degradation products. Migration positions of molecular weight markers (kDa) are indicated. (d) Phase-contrast images of cells from strain EG852, with vanillate-induced expression of *ftsZ* and xylose-induced expression of *ΔCTL*. Cells were grown for 17.5 h in M2 medium with the indicated inducer prior to imaging. Bar = 2 µm. (e) Growth of strain EG852 in M2 with the indicated inducers added at time 0, as monitored by optical density (OD) at 600 nm. Mean ± s.d. from three technical replicates is plotted. (f) Immunoblot of lysates of strain EG852 from (d) after 17.5 h growth in M2 with the indicated inducers and using FtsZ (top) or SpmX (bottom) antisera. Asterisks indicate degradation products. Migration positions of molecular weight markers (kDa) are indicated. (g, h) Merged phase contrast (blue) and fluorescence (yellow) images of strains EG990 and EG991, producing *cfp-ftsZ* (g) or *cfp-ΔCTL* (h), respectively, while depleting WT FtsZ for the indicated times. Bar = 2 µm.

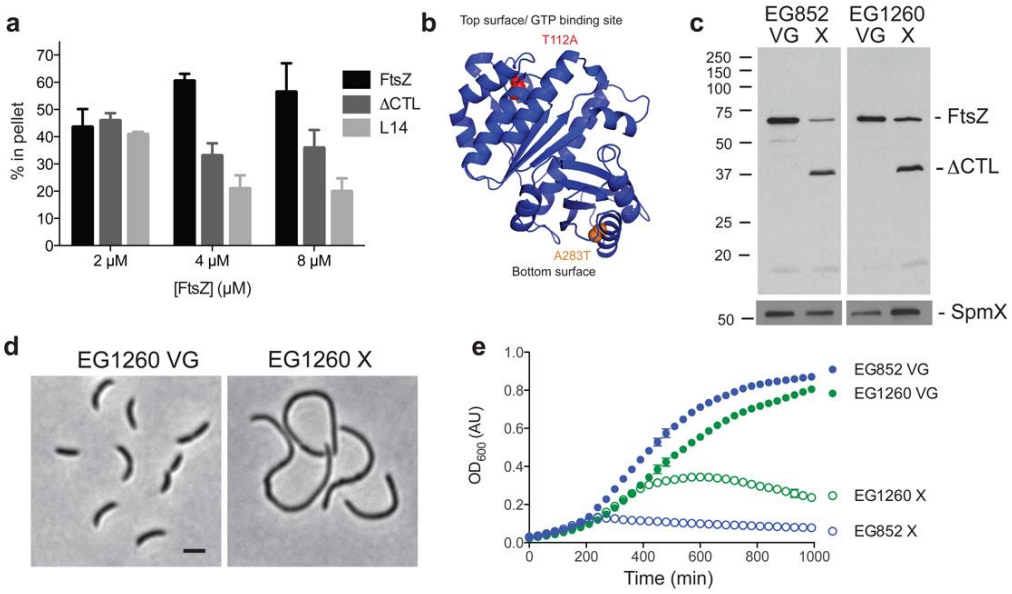

Supplementary Figure 5. ΔCTL must polymerize to cause bulging and lysis. (a) Fraction of FtsZ, ΔCTL, and L14 FtsZ variants in the pellet after high-speed centrifugation under polymerizing conditions. (b) Locations of suppressing mutations on a model of the structure of *Cc*FtsZ. Model includes residues 33-318 and was generated by SWISS-MODEL using PDB 2VXY (*B. subtilis* FtsZ at 1.7 Å resolution) as a template. (c) Immunoblot of lysates from strain EG852, bearing vanillate-induced *ftsZ* and xylose-induced *ΔCTL*, and strain EG1260, bearing vanillate-induced *ftsZ* and xylose-induced ΔCTL_{TA}, grown in PYE with vanillate and glucose (VG) or xylose (X) for 7.5 h. FtsZ (top) or SpmX (bottom) antisera were used. Migration positions of molecular weight markers (kDa) are indicated. (d) Phase contrast images of strains from (c) grown in PYE with the indicated inducers for 5 h. Bar = 2 μm. (e) Growth of strains EG1260 and EG852 in PYE with the indicated inducers added at time 0, as monitored by OD_{600}. Mean ± s.d. are plotted for three technical replicates.

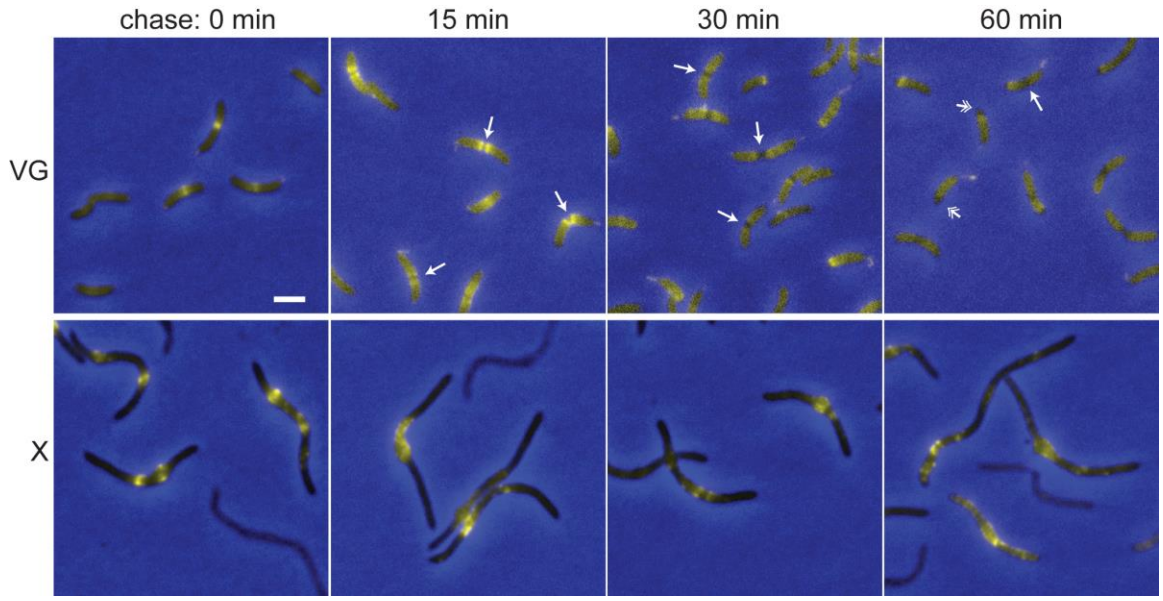

Supplementary Figure 6. Cell wall material persists at bulges for extended periods of time. Cells from strain EG852 were grown in the presence of vanillate and glucose (to induce *ftsZ*) or xylose (to induce *ΔCTL*) for 5 h prior to pulse labeling with HADA for 5 min. Cells were washed and allowed to grow without label for the indicated chase period prior to imaging. Merged fluorescence (yellow) and phase contrast (blue) images are shown. Clearing of HADA label (indicated by arrows) occurs quickly at midcell in cells producing FtsZ as new material is inserted and older material is moved longitudinally. No regular pattern of clearing of the HADA signal occurs in ΔCTL-producing cells, suggesting an altered pattern of PG metabolism. Bar = 2 µm.

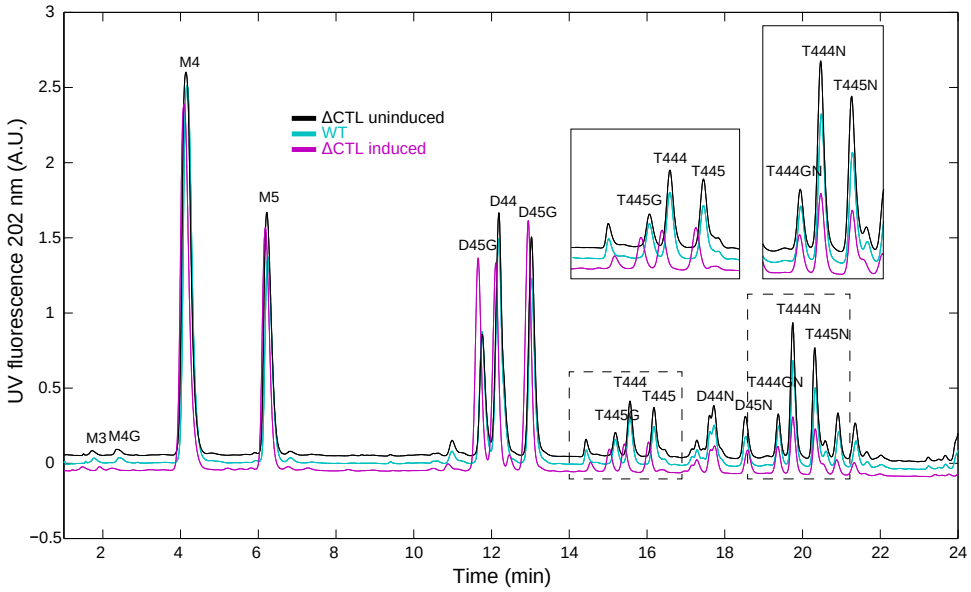

Supplementary Figure 7. Chromatograms of purified peptidoglycan sacculi from *C. crescentus* wildtype, ΔCTL uninduced, and ΔCTL induced strains. Strains (wildtype or EG852) were grown overnight, sacculi were purified and digested, and samples were analyzed using UPLC (see Methods). Chromatograms were overlaid and baselines were staggered, with the ΔCTL-induced chromatogram shifted to the left by 0.5 min for easier comparison. Highlighted regions identify the trimer peaks, showing a substantial reduction in the ΔCTL-induced strain as compared to the wildtype and ΔCTL uninduced strains. Peaks are labeled with the identity of the muropeptide species. M, monomer; D, dimer; T, trimer; 3, tripeptide; 4, tetrapeptide; 5, pentapeptide; G, terminal Gly; N, anhydro.

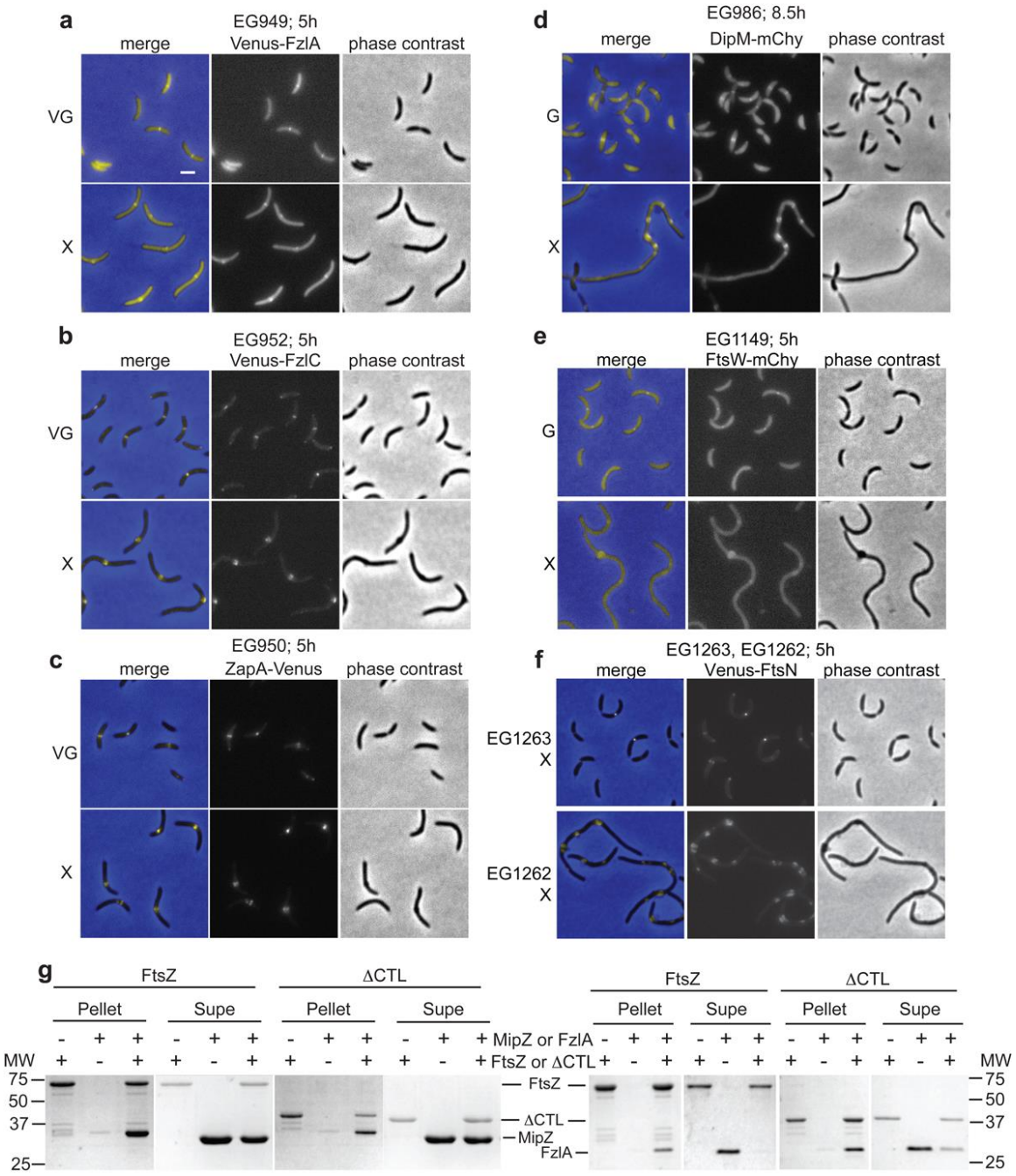

Supplementary Figure 8. Midcell proteins are recruited to sites of ΔCTL assembly.

Fluorescence, phase contrast, and merged images of fluorescent fusions to midcell-localized proteins in cells producing ΔCTL are shown. (a-c) Fluorescent fusions were produced constitutively from low-copy plasmids in a background with vanillate-induced

WT *ftsZ* and xylose-induced *ΔCTL*. *ΔCTL* was induced for 5 h prior to imaging. (d) *dipM-mCherry* was integrated at the *vanA* locus in a background with WT *ftsZ* under the control of its own promoter at its native locus and xylose-induced *ΔCTL*. *ΔCTL* was induced for 8.5 h and *dipM-mCherry* was induced for 2 h prior to imaging. (e) *ftsW-mCherry* was expressed from its own promoter at the *ftsW* locus. *ΔCTL* expression was induced from the *xylX* locus for 5 h. (f) *venus-ftsN* was integrated at the *xylX* locus in a background with xylose-induced *ΔCTL* also at the *xylX* locus (EG1262) or in a WT background (EG1263). Both genes were induced with xylose for 5 h prior to imaging. All proteins examined show enrichment at bulges. Bar = 2 µm. (g) Coomassie-stained SDS-PAGE of pellet and supernatant (supe) fractions after high-speed co-sedimentation of the indicated proteins. FtsZ or ΔCTL (3 µM) was polymerized with MipZ (9 µM, left) or FzlA (3 µM, right) prior to centrifugation at 250,000 x *g* for 15 min at 25^{o}C. MipZ promotes depolymerization of FtsZ while FzlA stabilizes FtsZ polymers; each retains its respective activity toward ΔCTL. Migration positions of molecular weight markers (kDa) are indicated.

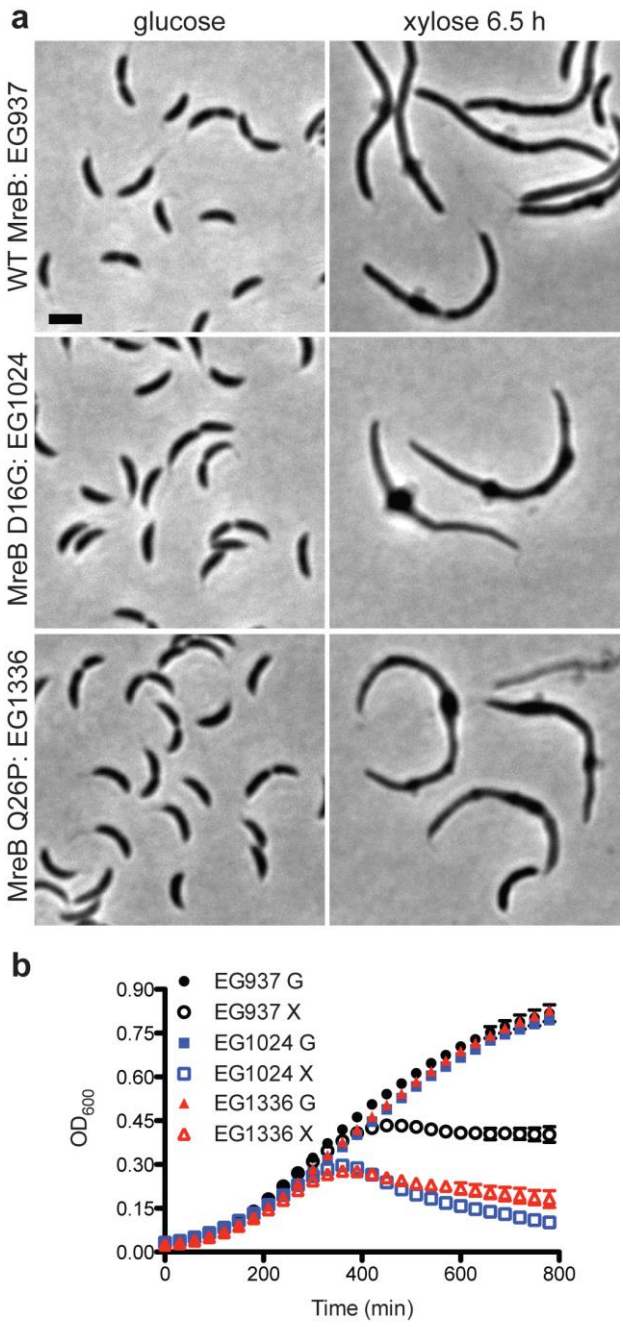

Supplementary Figure 9. Midcell MreB is not required for bulging and lysis. (a) Phase contrast images of the indicated strains grown with glucose or xylose (to induce *ΔCTL*) for 6.5 h. Bar = 2 µm. (b) Growth curves of strains from (a). Glucose (G) or xylose (X) was added at time 0. Mean ± s.d. from three technical replicates are shown.

Supplementary References

1. Möll, A. & Thanbichler, M. FtsN-like proteins are conserved components of the cell division machinery in proteobacteria. *Molecular Microbiology* **72**, 1037–1053 (2009).
2. Strobel, W., Möll, A., Kiekebusch, D., Klein, K.E., & Thanbichler, M. Function and localization dynamics of bifunctional penicillin-binding proteins in *Caulobacter crescentus*. *J. Bacteriol.* **196**, 1627-1639 (2014).
3. Thanbichler, M., Iniesta, A. A. & Shapiro, L. A comprehensive set of plasmids for vanillate- and xylose-inducible gene expression in *Caulobacter crescentus*. *Nucleic Acids Res.* **35,** e137 (2007).
4. Goley, E. D., Dye, N. A., Werner, J. N., Gitai, Z. & Shapiro, L. Imaging-based identification of a critical regulator of FtsZ protofilament curvature in *Caulobacter*. *Mol. Cell* **39,** 975–987 (2010).
5. Goley, E. D. *et al*. Assembly of the *Caulobacter* cell division machine. *Molecular Microbiology* **80,** 1680–1698 (2011).
6. Goley, E. D., Comolli, L. R., Fero, K. E., Downing, K. H. & Shapiro, L. DipM links peptidoglycan remodelling to outer membrane organization in *Caulobacter*. *Molecular Microbiology* **77,** 56–73 (2010).
7. Thanbichler, M. & Shapiro, L. MipZ, a spatial regulator coordinating chromosome segregation with cell division in *Caulobacter*. *Cell* **126**, 147–162 (2006).
8. Aaron, M. *et al.* The tubulin homologue FtsZ contributes to cell elongation by guiding cell wall precursor synthesis in *Caulobacter crescentus*. *Molecular Microbiology* **64,** 938–952 (2007).

9. Dye, N.A., Pincus, Z., Fisher, I.C., Shapiro, L., & Theriot, J.A. Mutations in the nucleotide binding pocket of MreB can alter cell curvature and polar morphology in *Caulobacter*. *Molecular Microbiology* **81**, 368-394.

10. Stephens, C., Mohr, C., Boyd, C., Maddock J, Gober, J. & Shapiro, L. Identification of the *fliI* and *fliJ* components of the *Caulobacter* flagellar type III protein secretion system. *J. Bacteriol*. **179,** 5355–5365 (1997).

11. Evinger, M. & Agabian, N. Envelope-associated nucleoid from *Caulobacter crescentus* stalked and swarmer cells. *J. Bacteriol.* **132**, 294–301 (1977).

12. Wang, Y., Jones, B. D. & Brun, Y. V. A set of *ftsZ* mutants blocked at different stages of cell division in *Caulobacter*. *Molecular Microbiology* **40,** 347–360 (2001).